UNIVERSITY of
BRADFORD

Library

The University of Bradford Institutional Repository

http://bradscholars.brad.ac.uk

Link to original published version: http://dx.doi.org/10.1049/iet-rpg.2015.0334

Citation: Mokryani G, Majumdar A and Pal BC (2016) A probabilistic method for the operation of three-phase unbalanced active distribution networks. IET Renewable Power Generation. 10(7): 944-954.

A Probabilistic Method for the Operation of Three-Phase Unbalanced Active Distribution Networks

Geev Mokryani[1], Ankur Majumdar[2], and Bikash C. Pal[2]

1. School of Electrical Engineering and Computer Science, University of Bradford, UK (e-mail:g.mokryani@bradford.ac.uk)
2. Department of Electrical and Electronic Engineering, Imperial College London, UK
(emails:ankur.majumdar@imperial.ac.uk, b.pal@imperial.ac.uk)

Abstract - **This paper proposes a probabilistic multi-objective optimization method for the operation of three-phase distribution networks incorporating active network management (ANM) schemes including coordinated voltage control and adaptive power factor control. The proposed probabilistic method incorporates detailed modelling of three-phase distribution network components and considers different operational objectives. The method simultaneously minimizes the total energy losses of the lines from the point of view of distribution network operators (DNOs) and maximizes the energy generated by photovoltaic (PV) cells considering ANM schemes and network constraints. Uncertainties related to intermittent generation of PVs and load demands are modelled by probability density functions (PDFs). Monte Carlo simulation method is employed to use the generated PDFs. The problem is solved using ε-constraint approach and fuzzy satisfying method is used to select the best solution from the Pareto optimal set. The effectiveness of the proposed probabilistic method is demonstrated with IEEE 13- and 34- bus test feeders.**

Keywords — **Photovoltaic cells, uncertainties, loss minimization, PV capacity, distribution network operators, unbalanced distribution network, Monte Carlo simulation.**

1. Introduction

Distribution network operators (DNOs) are incorporating the application of advanced metering and automation technologies into the networks with the notion of smart grids (SGs) implementation in power systems. The SGs include the technology that allows integrating and intelligently controlling these innovations [1]. Due to the environmental concerns and incentives from regulators, the SGs are assumed to integrate renewable distributed generators (DGs). However, the high penetration of renewable DGs such as wind and photovoltaics (PVs) introduces several impacts on distribution networks such as voltage rise, reverse power flow and voltage unbalance [2]. With increasing penetration of single phase rooftop PVs, phase domain study is needed for incorporating the load unbalance and network asymmetries as well as to evaluate the effects of single-phase PVs installed in three-phase distribution networks. Therefore, three-phase power flow should be utilized for network asymmetry analysis and load unbalance. Without the direct control of utilities over the sizes and locations of customer-installed rooftop PVs, improper placement of PVs will affect different phases of a feeder such as unbalanced effect of voltage rise and reverse power flow [3-4]. Unbalanced operation of three-

1

phase distribution networks can also influence induction motors and power electronic converters [5-6]. This paper proposes a probabilistic multi-objective methodology for assessing the amount of PV power that can be injected into the three-phase distribution network and the total energy losses of the lines taking into account active network management (ANM) schemes such as coordinated voltage control (CVC) and adaptive power factor control (PFC). The method simultaneously minimizes the total energy losses of the lines from the point of view of DNOs and maximizes the energy generated by PVs considering network constraints and uncertainties such as solar irradiance and load demand. The components modelling of three-phase distribution networks such as PVs, loads, lines and transformers are provided. The stochastic nature of solar irradiance and load demand are respectively modelled by Beta and Normal probability density functions (PDFs) and Monte Carlo simulation (MCS) method is utilized to use the generated PDFs. The problem is solved using ε-constraint method and fuzzy satisfying approach is used to select the best solution.

There are many references on operation of three-phase distribution networks which are explained in the following. A network based distribution slack bus model for DGs in unbalanced power flow studies is proposed in [7]. Scalar participation factors which reflect the network parameters, load allocation and generator capacities were applied to distribution uncertain system real power loss during power flow calculations. In [8], the authors proposed a continuation three-phase power flow method in polar coordinates for the voltage stability analysis. The formulation of three-phase power flow and modeling of synchronous machine are also developed. In [9], two methods have been proposed for three-phase power flow studies in which all component models are established in positive-negative-zero sequences. The first one is the bus admittance method which can be used as a benchmark to some extent and the second is the decoupling compensation method which is fast and accurate. A three-phase power-flow methodology in the sequence-component frame for the microgrid and active distribution network applications is proposed in [10]. The method accommodates unbalanced loads and lines, three/four-wire distribution lines and single-phase laterals. In [11], a three-phase power flow algorithm for distribution networks considering the three/four-wire configurations is proposed in order to more accurate evaluation of rooftop PV effects on different phases and neutrals. A three-phase transformer model is developed to interface between the 3-wire medium voltage and the 4-wire low voltage networks. In [12], an economic dispatch is proposed for unbalanced three-phase distribution networks to minimize the cost of imported power from the grid over a time horizon. The authors in [13] proposed a novel approach for the optimization of n-conductor systems taking into account the phase imbalances, different types of loads, neutral cables, groundings and other inherent characteristics of distribution systems. The formulation for the OPF of n-conductor system was developed using a primal–dual interior point method. A chance constrained OPF model is proposed in [14] taking into account forecast errors of renewable DGs for the operating of unbalanced three-phase distribution networks and *N-1* contingency. In [15], the authors proposed a distribution OPF in unbalanced distribution networks considering three-phase distribution network components representation. In [16], the authors proposed droop controlled islanded microgrids

optimal power flow (OPF) considering maximum loadability of the system. Balanced and unbalanced microgrids are used to investigate the loadability of the system. A two-stage reconfiguration method for minimisation of active power losses in balanced and unbalanced distribution systems is proposed in [17]. In the first stage, current information achieved from a power flow in a sequential manner. In the second stage, branch exchange operation is explored for further loss reduction.

In [18-22], the authors assumed that the distribution network is a balanced three-phase network, and therefore single-phase equivalents are utilized to decrease the computational burden. Nevertheless, due to unbalanced loads, untransposed three-phase feeders and presence of single-phase laterals, such an assumption cannot be realistic. Hence, it is necessary to take into account three-phase models of distribution networks components for more accurate operational decision. Table I summarizes a taxonomy of proposed methodologies for the optimization of unbalanced distribution networks. The gap that this paper tries to fill is as follows:

1) To model the uncertainties related to unbalanced Y and Δ load demands and solar irradiance in three-phase balanced PVs.

2) How the ANM schemes in three-phase framework can impact on the energy generated by PVs and energy losses of the lines.

To the best of our knowledge, no probabilistic method for evaluating the impact of ANM schemes on energy losses and energy generated by PVs in three-phase distribution networks has been reported in the literature. The method allows the assessment of the amount of PV power that can be injected into the grid and the energy losses can be reduced considering uncertainties and network constraints.

The modelling of abovementioned uncertainties in the operation of three-phase unbalanced distribution networks has not been taken into account. For example, in [12-17], the authors have not addressed the modelling of uncertainties related to load demand and renewable resources in three-phase framework. The method also integrates the ANM schemes into the methods and a comprehensive modelling of the three-phase unbalanced components is taken into account which is not addressed in the previous works [18-22]. Therefore, the main contributions of this paper are as follows:

1) To develop a decision-making framework for the operation of three-phase distribution networks considering ANM schemes.

2) To model three-phase distribution network components comprehensively.

3) To model uncertainties related to unbalanced loads and solar irradiance of three-phase balanced PVs.

4) To provide a tool to assist DNOs in evaluating the impact of PV integration in active distribution networks in terms of energy losses minimization and energy generated by PVs.

The rest of the paper is organized as follows. Section 2 explains the structure of the proposed method. Section 3 describes the modelling of three-phase distribution network components. The uncertainty modeling is discussed in Section 4. Problem

formulation is described in Section 5. Section 6 presents the IEEE 13- and 34 bus test feeders and simulation results. Conclusions are presented in Section 7.

Table I. Comparing proposed method with different existing methods

Reference	Single/Multi-objective	Uncertainty handling	Three-phase modelling	ANM schemes	Method
[12]	Single-objective	No	No	No	Semidefinite Relaxation
[13]	Single-objective	No	No	No	Primal dual interior point
[14]	Multi-objective	No	No	No	two-point estimate method
[15]	Multi-objective	No	Yes	No	Weighting factor
[16]	Multi-objective	No	Yes	No	Fuzzy approach
Proposed method	**Multi-objective**	**Yes**	**Yes**	**Yes**	**ε-constraint and Fuzzy approach**

2.   The Structure of the Proposed Method

The proposed probabilistic method is on the basis of MCS taking into account stochastic variations of solar irradiance and load demand. The method randomly generates solar irradiance and load demands from probability density functions (PDFs). For each combination of solar irradiance and load demand, different multi-objective optimizations are carried out to simultaneously minimize the total energy losses of the lines and maximize energy generated by PVs considering ANM schemes and network constraints. A quantitative probabilistic analysis of technical indicators such as total energy losses and energy generated by PVs can be achieved by the aggregate results of the MCS. The following steps are carried out by the proposed method as shown in Fig.1.
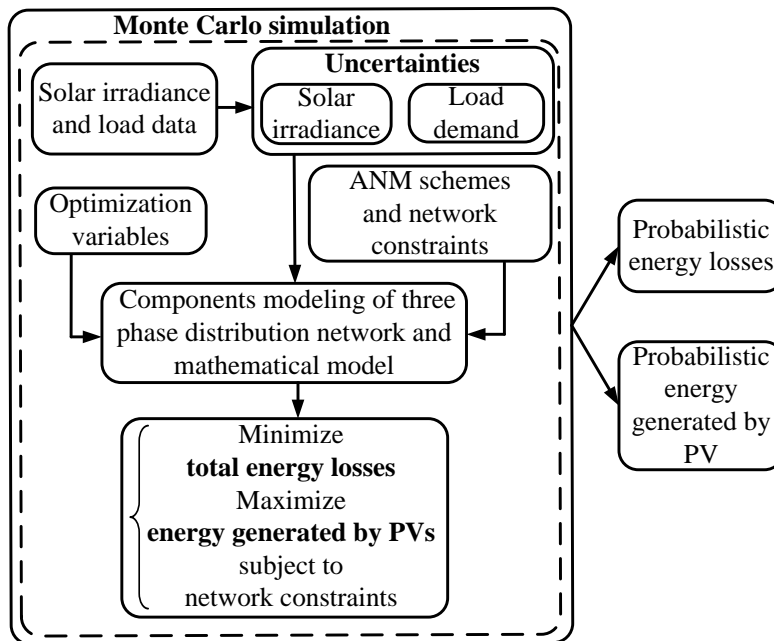

Fig.1.The structure of the proposed method

1) Set the candidate buses according to solar irradiance historical data [23-24]. It is assumed that the solar irradiance is the same for all phases.

2) Define the size of PVs and irradiance-power curves of three-phase balanced PVs.

3) Model the three-phase distribution network components such as PVs, loads, lines and transformers as described in Section 3.

4) Model the uncertainty related to solar irradiance for three-phase balanced PVs by using Beta PDF [25].

5) Derive the PDF of the three-phase PV's active power output on the basis of the Beta PDF of solar irradiance and irradiance to power conversion function of PVs as described in Section 4.A.

6) Model the uncertainties related to single-, two-, and three-phase unbalanced Y and Δ load demands by using Normal PDF for each phase [26] as explained in Section 4.B.

7) Perform MCS of length N (number of samples).

8) For each sample of MCS, simultaneously minimize total energy losses of the lines and maximize the energy generated by PVs considering ANM schemes and network constraints. The formulation of multi-objective optimization problem is described in Section 5.

9) The results of the proposed method provide the probabilistic energy generated by PVs and total energy losses.

3. Modelling the Three-Phase Distribution Network Components

The mathematical model of the components of three-phase distribution networks such as PVs, loads, lines and transformers are described in the following.

A. PV Modelling

Generally, DGs in distribution networks can be modelled as P-V, P-Q or P-Q-V models [27]. In this paper, the voltage, active and reactive power of PVs are control variables and it is assumed that PVs are balanced. The loads are unbalanced and has also single and two-phase laterals, the PVs are supposed to have independent three-phase control. Therefore, PVs are modelled as P-Q-V model with independent three-phase control.

B. Load Modelling

There are numerous types of balanced and unbalanced loads in distribution networks, in comparison with transmission networks, according to number of phases i.e. single-, two - or three-phase and connection types (Δ or Y). Furthermore, from the point of view

of electricity usage, constant power, constant current, constant impedance or any combination must be performed for the realistic load models. This model is usually denoted as ZIP model which is described for Δ and Y loads in equations (1), (2), respectively [28]. Single- and two-phase loads in both Y and Δ connected types are modelled by setting the missing phase to zero.

$$P_{ab}^{ZIP} = P_0(P_P + P_I \left| \frac{V_{ab}}{\sqrt{3}V_n} \right| + P_Z \left| \frac{V_{ab}}{\sqrt{3}V_n} \right|^2) , \ P_P + P_I + P_Z = 1 \quad (1a)$$

$$Q_{ab}^{ZIP} = Q_0(Q_P + Q_I \left| \frac{V_{ab}}{\sqrt{3}V_n} \right| + Q_Z \left| \frac{V_{ab}}{\sqrt{3}V_n} \right|^2) , Q_P + Q_I + Q_Z = 1 \quad (1b)$$

$$P_a^{ZIP} = P_0(P_P + P_I \left| \frac{V_a}{V_n} \right| + P_Z \left| \frac{V_a}{V_n} \right|^2) , \ P_P + P_I + P_Z = 1 \quad (2a)$$

$$Q_a^{ZIP} = Q_0(Q_p + Q_I \left| \frac{V_a}{V_n} \right| + Q_Z \left| \frac{V_a}{V_n} \right|^2) , Q_P + Q_I + Q_Z = 1 \quad (2b)$$

In this paper, for the sake of simplicity, it is assumed that the loads are voltage-independent and the constant impedance and constant current components are neglected; therefore, the loads are modeled as constant power. But, it can be extended to constant current and constant impedance as well. Regarding constant current and constant impedance loads, for each sample of MCS, the nominal power (power at nominal voltage) is taken from the Normal PDF, which is for nominal power. For that sample, at each iteration of the optimization process, the load power changes with change in the voltage. So, for the next iteration, the load power is calculated based on the voltage on that iteration. The process continues until convergence.

C. Line and Transformer Modelling

As the distribution networks consist of single, two and non-transposed three-phase lines and they often serve unbalanced loads, it is required to compute the impedances (both self and mutual impedances) of the lines as accurate as possible and consider the ground return path for the unbalanced currents.
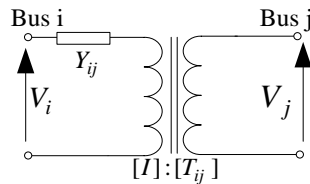

Fig.2. Model of a generic branch

The modified Carson's equation is utilized to characterize a line with conductors which are connected to a source at one end and grounded at the remote end [29].

In this paper, any three-phase line is modelled as a symmetrical π series with an ideal transformer with ratio $[I]:[T_{ij}]$, as shown in Fig.2. I, T_{ij} and Y are 3×3 identical, 3×3 diagonal and $(N_{bus}\times3)\times(N_{bus}\times3)$ matrices respectively, instead of a single element in case of balanced single-phase network. Y and T_{ij} are presented in equations (3) and (4), respectively. The transformers including on-load tap changers (OLTCs) and voltage regulators (VRs) are modelled as three single-phase transformers. The connection type of OLTCs and VRs is respectively Δ/Y and Y/Y. Moreover, it is assumed that transformers are ideal (i.e. no losses and similar impedances).

$$Y = \begin{bmatrix} Y_{11}^{aa} & Y_{11}^{ab} & Y_{11}^{ac} & \cdots\cdots & Y_{1n}^{aa} & Y_{1n}^{ab} & Y_{1n}^{ac} \\ Y_{11}^{ba} & Y_{11}^{bb} & Y_{11}^{bc} & \cdots\cdots & Y_{1n}^{ba} & Y_{1n}^{bb} & Y_{1n}^{bc} \\ Y_{11}^{ca} & Y_{11}^{cb} & Y_{11}^{cc} & \cdots\cdots & Y_{1n}^{ca} & Y_{1n}^{cb} & Y_{1n}^{cc} \\ : & : & : & \cdots\cdots & : & : & : \\ Y_{n1}^{aa} & Y_{n1}^{ab} & Y_{n1}^{ac} & \cdots\cdots & Y_{nn}^{aa} & Y_{nn}^{ab} & Y_{nn}^{ac} \\ Y_{n1}^{ba} & Y_{n1}^{bb} & Y_{n1}^{bc} & \cdots\cdots & Y_{nn}^{ba} & Y_{nn}^{bb} & Y_{nn}^{bc} \\ Y_{n1}^{ca} & Y_{n1}^{cb} & Y_{n1}^{cc} & \cdots\cdots & Y_{nn}^{ca} & Y_{nn}^{cb} & Y_{nn}^{cc} \end{bmatrix}_{(N_{bus}\times3)\times(N_{bus}\times3)} \quad (3)$$

$$T_{ij} = \begin{bmatrix} T_{ij}^{a} & 0 & 0 \\ 0 & T_{ij}^{b} & 0 \\ 0 & 0 & T_{ij}^{c} \end{bmatrix} \quad (4)$$

4. Uncertainty Modeling

A. Output Power of Three-Phase Solar Generating Sources

The generated power of a PV module relies on three parameters, namely, solar irradiance, ambient temperature of the site and the characteristics of the module itself. The Authors in [30-32] showed that solar irradiance generally follows Beta PDF; therefore, in this paper, the solar irradiance is modelled using a Beta PDF at each phase which is described as follows:

$$PDF(s,p) = \begin{cases} \dfrac{\Gamma(\alpha^p+\beta^p)}{\Gamma(\alpha^p)+\Gamma(\beta^p)} \times s_p^{\alpha-1} \times (1-s_p)^{\beta-1}, & \text{if} \quad 0\le s_p \le 1, 0\le \alpha^p, \beta^p \\ 0, & \text{else} \end{cases} \quad (5)$$

where s_p represents the solar irradiance (kW/m^2) at phase p and α^p, β^p are the parameters of beta PDF at each phase. In order to calculate the parameters of Beta PDF at each phase, the mean (μ^p) and standard deviation (σ^p) of the random variable at each phase are utilized as follows:

$$\beta^p = (1-\mu^p) \times \left(\frac{\mu^p \times (1+\mu^p)}{(\sigma^p)^2} - 1\right) \quad (6)$$

7

$$\alpha^p = \frac{\mu^p \times \beta^p}{1 - \mu^p} \tag{7}$$

The irradiance to power conversion function is used in this paper as follows [33]:

$$P_g(s, p) = \eta^g \times A^g \times s_p \tag{8}$$

where $P_g(s, p)$ represents PV output power (kW) for irradiance s_p at phase p; η^g and A^g are the efficiency (%) and total area (m^2) of PV system, respectively. According to the given irradiance distribution and irradiance to power conversion function, the PV power distribution is obtained. In this paper, it is assumed that the solar irradiance at all phases is the same and therefore the output power at all phases is the same.

B. Load Demand Uncertainty

In [34], the authors showed the load demand follows Normal PDF. For this reason, in this paper the three-phase unbalanced Y and Δ loads at each bus and each phase are modelled by Normal PDF as follows:

$$PDF(S_i^{L,p}) = \frac{1}{\sqrt{(2\pi\sigma_i^{L,p})}} \exp([\frac{(S_i^{L,p} - \mu_i^{L,p})^2}{2(\sigma_i^{L,p})^2}])$$

$$p = \begin{cases} a,b,c & \text{For Y loads} \\ ab,bc,ca & \text{For } \Delta \text{ loads} \end{cases} \tag{9}$$

where $S_i^{L,p}$, $\mu_i^{L,p}$ and $(\sigma_i^{L,p})^2$ are respectively the apparent power, the mean and variance of the load demands at bus i and phase p. In order to calculate the active and reactive power at each line of Δ loads, the following steps are carried out. The Y equivalent powers for Δ loads are calculated in each iteration from equations (10)-(13).

1) Calculate line voltage of Δ loads.

$$\begin{bmatrix} V_i^{ab} \\ V_i^{bc} \\ V_i^{ca} \end{bmatrix} = \begin{bmatrix} V_i^a \angle \theta^a - V_i^b \angle \theta^b \\ V_i^b \angle \theta^b - V_i^c \angle \theta^c \\ V_i^c \angle \theta^c - V_i^a \angle \theta^a \end{bmatrix} \tag{10}$$

2) Obtain active and reactive power of Δ loads.

3) Calculate line currents of Δ loads as follows.

$$I_{ab} = (\frac{P_{ab} - jQ_{ab}}{V_{ab}\angle\theta_{ab}})^* \tag{11}$$

4) Calculate the current at each phase according to the following equation.

$$\begin{bmatrix} I_a \\ I_b \\ I_c \end{bmatrix} = \begin{bmatrix} 1 & 0 & -1 \\ -1 & 1 & 0 \\ 0 & -1 & 1 \end{bmatrix} \begin{bmatrix} I_{ab} \\ I_{bc} \\ I_{ca} \end{bmatrix} \tag{12}$$

5) Calculate the active and reactive power at each phase as follows.

$$\begin{aligned}
S_a &= V_a I_a^* = P_a + jQ_a \\
S_b &= V_b I_b^* = P_b + jQ_b \\
S_c &= V_a I_a^* = P_c + jQ_c
\end{aligned} \tag{13}$$

5. Problem Formulation

A. Objective Functions

Energy losses minimization have positive effects in distribution networks such as voltage drop reduction, voltage profile improvement and other economic and environmental advantages. However, from the point of view of DNOs, it is essential to evaluate the available distribution network capacity in terms of renewable DG penetration without needing extra investments in the network. Therefore, based on these considerations, the objective of the proposed problem is jointly minimizing the total energy losses of the lines from the point of view of DNOs and maximizing the energy generated by PVs considering ANM schemes subject to network constraints as described in the following.

$$\text{Maximize } f_{obj} = f_1 - f_2 \tag{14}$$

$$f_1 = \sum_{\substack{p= \\ a,b,c}} \sum_g \sum_t P_{g,t}^p$$

$$f_2 = \sum_{\substack{p= \\ a,b,c}} \sum_i \sum_j \sum_t G_{ij}^{pp}\left((V_{i,t}^p)^2 + \frac{(V_{j,t}^p)^2}{(T_{ij}^p)^2} - 2\frac{V_{i,t}^p V_{j,t}^p \cos(\theta_{i,t}^p - \theta_{j,t}^p)}{T_{ij}^p}\right)$$

where f_{obj} is the total objective function. The first objective function is the total energy generated by the PVs at generator buses and the second one is the total active energy losses of the lines (where the maximization of minus energy losses is equal to its minimization). G_{ij}^{pp} is the conductance of the lines connecting bus i at phase p and bus j at phase p where $p \in \{a,b,c\}$. As there is no physical connection between bus i at phase p and bus j at phase m, therefore, there is no current flow between them. $P_{g,t}^p$ is the generated active power at generator buses and phase p and time t; $V_{i,t}^p$, $\theta_{i,t}^p$ and $V_{j,t}^m$, $\theta_{j,t}^m$ are voltage and voltage angle at buses i and j and phases p and m and time t, respectively. t is the number of hours over a year which is equal to number of samples. Note that in the sampling procedure, the possible sampling values are generated on hourly basis and a year is equal to 8760 sampling hours.

B. ANM Schemes Incorporation

DNOs will be able to optimize using their assets with incorporation of ANM schemes by dispatching generation, controlling OLTCs and voltage regulators, controlling reactive power, and reconfiguring the system [35]. ANM implementations will need advanced control techniques while the actual actuation of devices (e.g., tap changers) will depend on their respective response time-scales.

1) Coordinated Voltage Control

In general, passive networks set the substation secondary voltage to a fixed value (e.g., 1.05 p.u.), and operate DGs at constant power factors (e.g., $\cos(\phi_g)=0.95$, leading or lagging) in different load conditions. In fact, DNOs may vary the target distribution voltage seasonally to provide for voltage drops during maximum load while ensuring excessive voltage rise does not occur where DGs exist. By coordination of the reactive power operation of DGs with the substation target voltage, the overall performance of the system can be considerably increased [36]. Here, the voltage at the substation secondary is considered as a variable and for the coordinated voltage control, the secondary voltage of the OLTC is treated as a variable while maintaining its value within the statutory range. Therefore, the following constraint applies:

$$T_{ij}^{\min} \leq T_{ij}^{p} \leq T_{ij}^{\max} \tag{15}$$

where T_{ij}^{p} is the tap magnitude of OLTC at each phase, $T_{ij}^{\min}$ and $T_{ij}^{\max}$ are respectively lower and upper limits they can assume.

2) Adaptive Reactive Power Control

DGs usually operate at constant power factors that present most benefit for active power generation. Nevertheless, recent grid codes for DG connections require that actual reactive power capabilities are significant (for example $\cos(\phi_g)=0.90$ inductive/capacitive). DGs, by incentive or by requirement, could operate at a pre-defined fixed power factor that minimizes reactive support from the transmission grid considering network constraints. Operation of DGs at leading, unity or lagging power factors, depending on the technology utilized, is feasible. Nevertheless, the ability of DGs to offer dispatchable or adaptive power factor control depends on the existence of a proper ancillary service market or through requirements in the connection agreement [37]. Here, it is conceived that PVs provide such a scheme with the power angle of each PV considered as optimization variable. In fact, PVs will be required to operate within a certain range of power factors, therefore the following constraint applies:

$$\phi_{g}^{\min} \leq \phi_{g,t}^{p} \leq \phi_{g}^{\max} \tag{16}$$

where $\phi_{g,t}^{p}$ is the power factor angle of PVs at phase p and time t, and $\phi_{g}^{\min} / \phi_{g}^{\max}$ are min/max values of power factor angle.

C. Capability Curve of PV Inverters

Fig. 3 shows the capability curve of PV inverters which includes manufacturing constraints and limitations defined by the DNO. The x- and y- axes are respectively the reactive and active power in p.u.. The dashed line is the power limit of the inverter. The inverter cannot operate outside this curve since it is limited by the nominal power of the PV. Note that the injected power is limited by the nominal current of the inverter, i.e. it is impossible to operate at maximum active and reactive power at the same time. The dash-dotted line is the limit of the active power injection by the PVs due to the power factor which is 0.95 here. The inverter can supply reactive power within the specified limits, i.e. Q_{min} and Q_{max}. In the dashed area, the inverter should supply reactive power within the specified power factor limits.
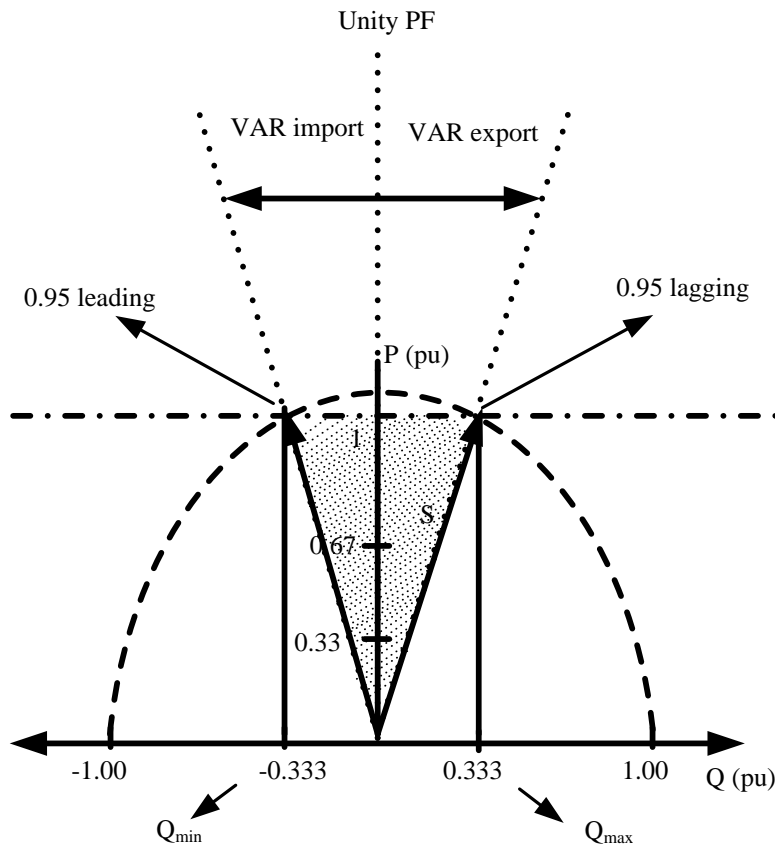

Fig.3. Capability curve of PV inverter

D. Network Constraints

a) Equality Constraints: Active and reactive power balance at each bus and phase p

$$P_{i,t}^{G,p} - P_{i,t}^{L,p} =$$

$$\sum_{\substack{m=\\a,b,c}} \left[\sum_{j=1}^{N_{bus}} V_{i,t}^p V_{j,t}^m T_{ij}^p \left[G_{ij}^{pm} \cos(\theta_{i,t}^p - \theta_{j,t}^m) + B_{ij}^{pm} \sin(\theta_{i,t}^p - \theta_{j,t}^m) \right] \right] \qquad (17)$$

$$\forall \, p \in \{a,b,c\}, p \neq m$$

$$Q_{i,t}^{G,p} - Q_{i,t}^{L,p} =$$

$$\sum_{\substack{m=\\a,b,c}} \left[\sum_{j=1}^{N_{bus}} V_{i,t}^p V_{j,t}^m T_{ij}^p \left[G_{ij}^{pm} \sin(\theta_{i,t}^p - \theta_{j,t}^m) - B_{ij}^{pm} \cos(\theta_{i,t}^p - \theta_{j,t}^m) \right] \right] \qquad (18)$$

$$\forall \, p \in \{a,b,c\}, p \neq m$$

where $P_{i,t}^{G,p} - P_{i,t}^{L,p}$ and $Q_{i,t}^{G,p} - Q_{i,t}^{L,p}$ are respectively the net active and reactive power injected at bus i and phase p, G_{ij}^{pm} and B_{ij}^{pm} are respectively the real and imaginary part of each element of admittance matrix (Y) which is $(N_{bus} \times 3) \times (N_{bus} \times 3)$ matrices, N_{bus} is the number of buses, $(\theta_{i,t}^p - \theta_{j,t}^m)$ is the difference in voltage angle between bus i and bus j at phases p and m, respectively, T_{ij}^p is the tap magnitude of OLTC at phase p.

b) Inequality Constraints

-Branch flow constraints at each phase

$$I_{ij}^a = \sqrt{((G_{ij}^{aa})^2 + (B_{ij}^{aa})^2)[(V_{i,t}^a)^2 + \frac{(V_{j,t}^a)^2}{(T_{ij}^a)^2} - 2\frac{V_{i,t}^a V_{j,t}^a \cos(\theta_{i,t}^a - \theta_{j,t}^a)}{T_{ij}^a}} \leq I_{ij}^{\max}$$

$$I_{ij}^b = \sqrt{((G_{ij}^{bb})^2 + (B_{ij}^{bb})^2)[(V_{i,t}^b)^2 + \frac{(V_{j,t}^b)^2}{(T_{ij}^b)^2} - 2\frac{V_{i,t}^b V_{j,t}^b \cos(\theta_{i,t}^b - \theta_{j,t}^b)}{T_{ij}^b}} \leq I_{ij}^{\max} \qquad (19)$$

$$I_{ij}^c = \sqrt{((G_{ij}^{cc})^2 + (B_{ij}^{cc})^2)[(V_{i,t}^c)^2 + \frac{(V_{j,t}^c)^2}{(T_{ij}^c)^2} - 2\frac{V_{i,t}^c V_{j,t}^c \cos(\theta_{i,t}^c - \theta_{j,t}^c)}{T_{ij}^c}} \leq I_{ij}^{\max}$$

where $I_{ij}^{\max}$ is the maximum current flow.

-Voltage limits at each bus and phase [38]

$$V_i^{\min} \leq V_{i,t}^p \leq V_i^{\max} \qquad (20)$$

$$\theta_i^{\min} \leq \theta_{i,t}^p \leq \theta_i^{\max} \qquad (21)$$

where $V_{i,t}^p$ and $\theta_{i,t}^p$ are respectively the voltage magnitude and voltage angle at bus i, phase p and time t, $V_i^{\min}/V_i^{\max}$ and $\theta_i^{\min}/\theta_i^{\max}$ represent the *min/max* values they can assume.

-PV generation constraint at each phase

$$P_{g,t}^{\min} \le P_{g,t}^{p} \le P_{g,t}^{\max} \qquad\qquad\qquad (22)$$

$$Q_{g,t}^{\min} \le Q_{g,t}^{p} \le Q_{g,t}^{\max} \qquad\qquad\qquad (23)$$

where $P_{g,t}^{p}$ and $Q_{g,t}^{p}$ are respectively generated active and reactive powers by PV at each bus and phase p and time t; $P_{g,t}^{\min} / P_{g,t}^{\max}$ and $Q_{g,t}^{\min} / Q_{g,t}^{\max}$ represent the *min/max* values they can assume at time t.

-Capacity constraints at slack bus and each phase

$$P_{b}^{\min} \le P_{b,t}^{p} \le P_{b}^{\max} \qquad\qquad\qquad (24)$$

$$Q_{b}^{\min} \le Q_{b,t}^{p} \le Q_{b}^{\max} \qquad\qquad\qquad (25)$$

where $P_{b,t}^{p}$ and $Q_{b,t}^{p}$ are active and reactive powers at the slack bus and phase p and time t, respectively; $P_{b}^{\min} / P_{b}^{\max}$ and $Q_{b}^{\min} / Q_{b}^{\max}$ represent the *min/max* values they can assume.

E. Solution Procedure

The proposed multi-objective optimization problem is solved through the ε-constraint approach that is an effective procedure to solve the problems with nonconvex Pareto front. This approach sets an upper limit for one objective function and minimizes the other one. This limit is gradually decreased and the Pareto front is achieved. The selection of the best solution of the Pareto optimal front is carried out by fuzzy satisfying approach [39] (see Appendix A).

6. Case Study and Simulation Results

A. IEEE 13-bus Test Feeder

In this section, the distribution system used to test the proposed method is described. The following analyses are based on a 13-bus IEEE test system whose data are given in [40]. The single line diagram of the distribution system is shown in Fig. 4. The number of phases is shown with cross bars in the feeders. It is assumed that transformers including OLTCs and VRs are ideal and modelled as three single-phase transformers as well as their connection type are respectively Δ/Y and Y/Y. The OLTC and VR have a target voltage of 1.05 p.u. at the secondary at all phases. Voltage limits at all phases are taken to be ±10% of nominal value, i.e. $V_{\min}$= 0.9 and $V_{\max}$= 1.1 p.u. and the thermal limits of the lines are 1.5 MVA. It is assumed that three 1.5 MW three-phase balanced PVs are installed at buses 3, 6 and 7 as shown in Fig. 4. Each phase of PVs is composed of $50 \times 10\,\mathrm{kW}$ solar panels with $\eta^{g} = 18.6\%$ and $A^{g} = 100\,\mathrm{m}^{2}$. The Beta PDF parameters of the solar irradiance at all phases are assumed to be α= 6.5, β = 3.5. The

average hourly solar irradiance at all phases and the histogram of the Beta PDF of the considered solar irradiance are shown in Figs. 5 (a), 5(b), respectively.
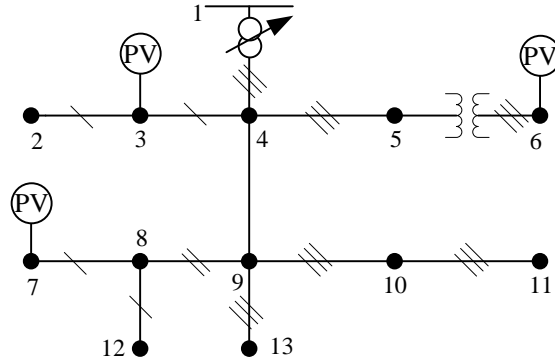

Fig.4. IEEE 13-bus distribution network

Each load is assumed to be a constant power load and the random load scenarios are generated using a typical load profile and modelled by Normal PDF. Usually, in distribution network studies, the same hourly randomly generated load profiles for all buses are considered but as the behavior of loads responds to external inputs, therefore, in this paper it is assumed that the randomly generated load profiles are not the same at all buses. The load data are assumed to be peak loads as provided in [29] and the typical load profile at each phase [41] is used as shown in Fig. 5(c). The histogram of the PDF of load demand at phase b and bus 3 is shown in Fig. 5(d). The mean and standard deviation for all Y and Δ loads are provided in Tables II. Equations (10)-(13) are used in order to calculate the active and reactive power at each line of Δ loads and the Y equivalent powers for Δ loads are calculated in every iteration. The stochastic load demand and solar irradiance vary on hourly basis corresponding to 8760 samples of the MCS over a year as this value allows satisfying the required degree of confidence with a reasonable computing time. Note that the possible sampling values are generated based on hourly basis which 8760 sampling hours is equal to a year. The method is on the basis of MCS technique considering different combinations of solar irradiance and load demand. The proposed method is applied to the abovementioned distribution network and implemented in GAMS [42] and solved using KNITRO solver [43] on a PC with Core i7 CPU and 16 GB of RAM.
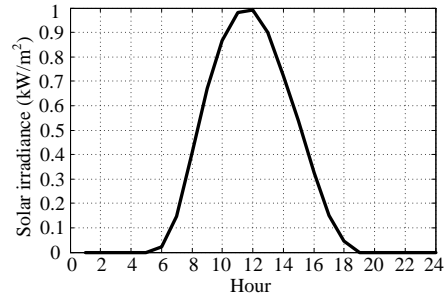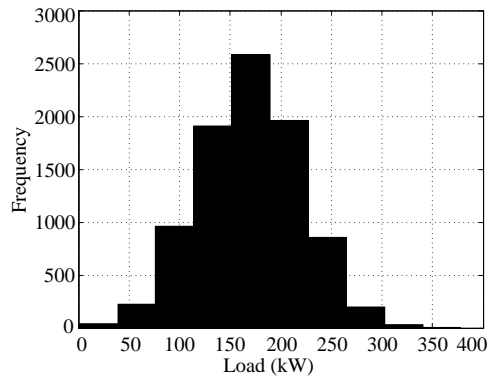
(a)
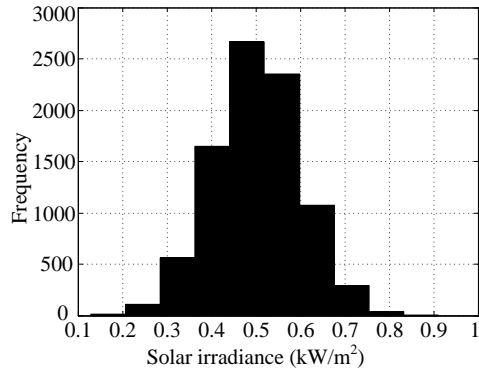
(b)
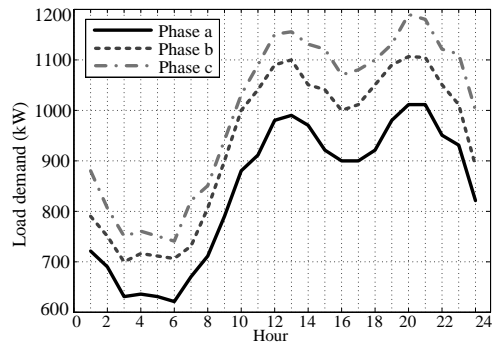
(c)

(d)

Fig.5. (a) hourly solar irradiance, (b) histogram of solar irradiance, (c) Load profile at each phase, (d) histogram of load at phase b of bus 3

Table II. Mean and Standard Deviation of Y and Δ Loads

Y loads						
Load No.	Mean (μ) (kW) at phases			Standard deviation (σ) (kW) at phases		
	a	b	c	a	b	c
3	-	170	-	-	50	-
6	160	120	120	40	20	20
7	-	-	170	-	-	50
11	485	68	290	120	10	110
12	128	-	-	30	-	-
Δ Loads						
Load No.	Mean (μ) (kW) between phases			Standard deviation (σ) (kW) between phases		
	ab	bc	ca	ab	bc	ca
2	-	230	-	-	50	-
9	385	385	385	110	110	110
10	-	-	170	-	-	50

In order to solve the multi-objective problem by ε-constraint method, maximum and minimum values of total energy losses (i.e. f_2) are calculated. These values are obtained by maximizing and minimizing each objective function individually as the total objective function.

So, by assuming as a constraint of the multi-objective optimization problem (in the form of $f_2 \geq \varepsilon$), lower bound of f_2 (i.e., ε) varies from 45.11 to 49.78 kWh and is minimized as the sole objective function of multi-objective problem. The Pareto optimal front of the two objective functions is derived which consists of 16 solutions. Table III shows the values of both objective functions in scenario *A* for all 16 Pareto optimal solutions. As explained in Section 6, in order to select the best solution among the obtained Pareto optimal sets, fuzzy satisfying method is used. It is obvious from the last column of Table III that the best solution is *Solution#9*, with the maximum weakest membership function of 0.624. The corresponding energy generated by PVs and energy losses are respectively equal to 3.69 MWh and 48.13 kWh.

In order to investigate the impact of ANM schemes on total energy generated by PVs and energy losses, three different scenarios are taken into account as presented in Table IV. The scenarios consider various combinations of ANM schemes. Scenario *A* is referred to passive management case (base case) which no CVC and PFC are considered and it is assumed that PVs operate at

power factor of 0.95 lagging. While in scenario *B*, only CVC is taken into consideration and in scenario *C*, both CVC and PFC are considered.

Table III. Pareto Optimal Solutions for IEEE 13-bus test feeder in Scenario *A*

Solution #	f_1 (MWh)	f_2 (kWh)	$\dfrac{f_1^{\max} - f_k}{f_1^{\max} - f_1^{\min}}$	$\dfrac{f_2^{\min} - f_k}{f_2^{\min} - f_2^{\max}}$	Min
1	2.69	45.11	1	0	0
2	2.72	45.78	0.999	0.102	0.102
3	2.87	46.12	0.912	0.205	0.205
4	2.99	46.19	0.893	0.355	0.355
5	3.01	46.22	0.813	0.461	0.461
6	3.21	46.53	0.792	0.494	0.494
7	3.51	47.29	0.751	0.522	0.522
8	3.65	47.38	0.711	0.596	0.596
9	**3.69**	**48.13**	**0.696**	**0.624**	**0.624**
10	3.75	48.19	0.611	0.711	0.611
11	3.81	48.83	0.522	0.759	0.522
12	3.85	48.99	0.436	0.832	0.436
13	4.21	49.11	0.365	0.896	0.365
14	4.41	49.25	0.296	0.911	0.296
15	4.59	49.66	0.152	0.971	0.152
16	4.61	49.78	0	1	0

Table IV. Scenarios

Scenarios	CVC	PFC	PF= 0.95 lagging
A	-	-	✓
B	✓	-	✓
C	✓	✓	-

The mean of dispatched energy and the loads at each phase and candidate buses in scenario *A* are shown in Figs. 6(a), (b), respectively. It is obvious that bus 6 and phase b has the lower dispatched energy compared to that at phases *a* and *c* due to the lowest amount of load at this phase. The amount of PV power that can be injected into the network is mainly limited by the voltage and thermal limits.The dispatched energy at bus 7 and phase *c*, is lower than that at bus 6 while the load at bus 7 is higher than that at bus 6. This is essentially because of lower voltage at bus 6 compared to that at bus 7 and the lower thermal limits of line 5-6 than that of 7-8. At bus 3 there is no load at phases *a* and *c*, therefore, no energy has been generated at these phases. This bus has the

lowest amount of energy generated by PVs compared to other buses and phases. This is mainly due to the lowest voltage and thermal limits of this bus compared to other buses and the lines connecting bus 3 compared to other lines, respectively.
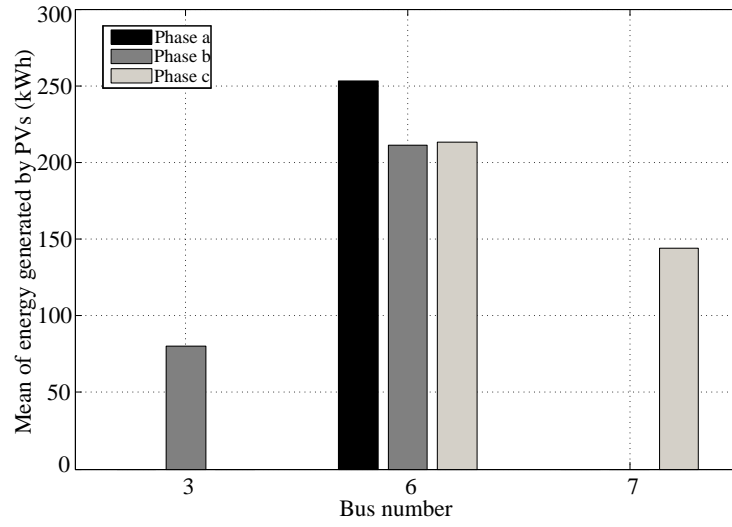
(a)
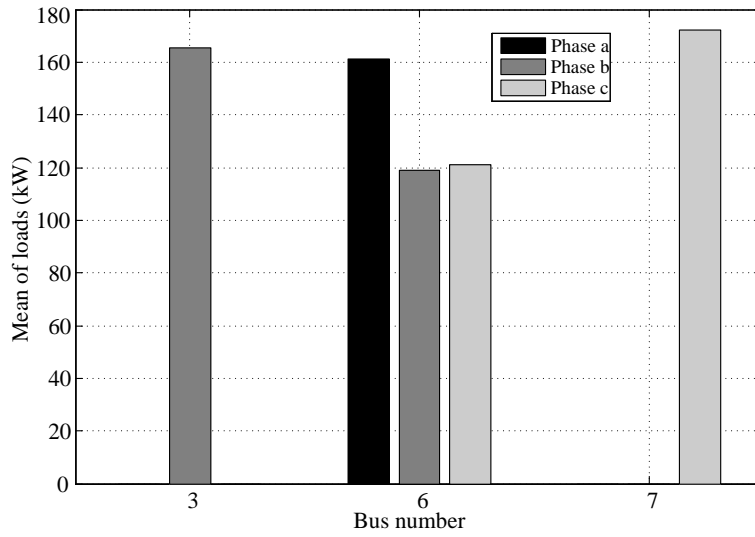
(b)

Fig.6. (a) Mean of energy generated by PVs at each phase and candidate buses in scenario *A*, (b) Mean of three-phase unbalanced loads at some buses and each

phase

B. IEEE 34-bus Test System

Simulations are also carried out on IEEE 34-bus test feeder [41] which is shown in Fig. 7. The provided load data are considered to be peak loads, load profiles and load modelling at each node are defined using the same approach used in the previous test system. It is assumed that five 1.5 MW three-phase balanced PVs are installed at buses {808, 822,826,846, 860}. The loads are also assumed to be constant power. Note that the size and parameters for modelling PVs are the same as those in the previous case.
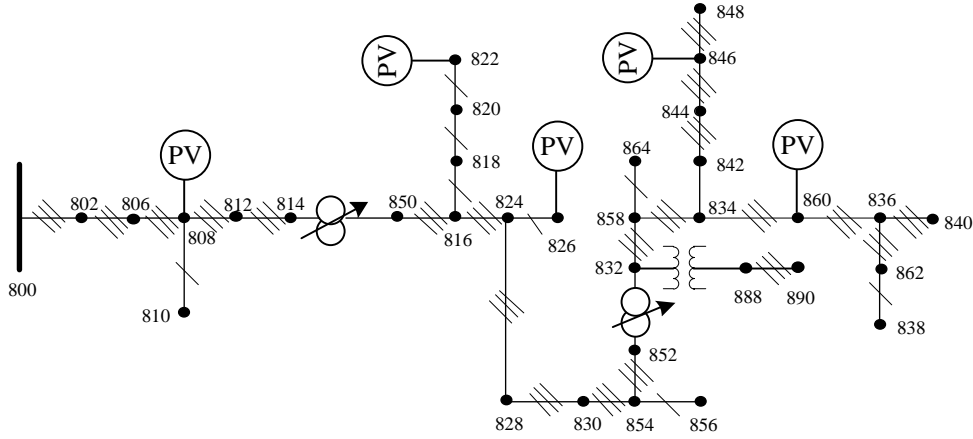

Fig.7. IEEE 34-bus test system

Table V presents the values of both objective functions in scenario *A* for all 30 derived Pareto optimal solutions. It is obvious from that the best solution is *Solution#22*, with the maximum weakest membership function of 0.697. The corresponding energy generated by PVs and energy losses are respectively equal to 4.77 MWh and 230.11 kWh.

Table V. Pareto Optimal Solutions for IEEE 34-bus test feeder in scenario *A*

| Solution #	f_1 (MWh)	f_2 (kWh)	$\dfrac{f_1^{\max} - f_k}{f_1^{\max} - f_1^{\min}}$	$\dfrac{f_2^{\min} - f_k}{f_2^{\min} - f_2^{\max}}$	Min
1	3.79	203.10	1	0	0
2	3.84	204.52	0.998	0.113	0.113
3	3.87	205.68	0.994	0.156	0.156
4	3.91	207.51	0.991	0.221	0.221
5	3.94	208.74	0.989	0.255	0.255
6	4.01	209.32	0.984	0.312	0.312
7	4.11	211.25	0.981	0.397	0.522
8	4.18	213.63	0.979	0.415	0.415
9	4.22	214.58	0.912	0.426	0.426
10	4.25	215.98	0.852	0.489	0.489
11	4.31	216.64	0.841	0.503	0.503
12	4.37	217.17	0.811	0.516	0.516
13	4.40	218.38	0.879	0.529	0.529
14	4.46	220.37	0.855	0.537	0.537
15	4.52	221.29	0.836	0.554	0.554
16	4.59	223.56	0.820	0.576	0.576
17	4.60	225.31	0.812	0.589	0.589
18	4.61	226.43	0.803	0.598	0.598
19	4.64	227.01	0.788	0.618	0.618
20	4.66	228.36	0.773	0.637	0.637
21	4.69	229.54	0.757	0.655	0.655
22	**4.77**	**230.11**	**0.723**	**0.697**	**0.697**
23	4.78	231.56	0.689	0.711	0.689
24	4.79	232.12	0.644	0.756	0.644
25	4.81	233.56	0.518	0.823	0.518
26	4.82	234.36	0.493	0.869	0.493
27	4.86	235.91	0.372	0.912	0.372
28	4.89	236.21	0.255	0.956	0.255
29	4.90	237.64	0.110	0.995	0.110
30	4.96	238.13	0	1	0

The mean of total dispatched energy in different scenarios over a year for both IEEE 13- and 34 bus test feeder is presented in the second column of Table VI. It is seen that the total dispatched energy with no ANM scheme in IEEE 13-bus test feeder is about 3.7 MWh while in scenario *B*, this value is about 3.9 MWh, thus, the dispatched energy increases about 5% compared to that in scenario *A*. The impact of using both ANM schemes including CVC and PFC on the total dispatched energy is evident. In scenario *C*, the total energy is almost 4.5 MWh, thus, it increases about 22% (as presented in the fourth column of Table VI) compared to that with no ANM schemes. The mean of total energy losses over a year in different scenarios is presented in the third column of Table VI. It is obvious that in scenario *A*, the energy loss is about 48 kWh while this value in scenario *C* is about 39 kWh. Energy losses decrease about 20% when considering both ANM schemes compared to that with no ANM scheme (see the fifth column of Table VI).

It is also seen that the energy generated by PVs for IEEE 34 bus test feeder in scenario *C* has highest value and the lines losses has the lowest value compared to those in scenario *A*. Therefore, by adopting both ANM schemes (scenario *C*), energy generated by PVs increases about 13% and energy losses decrease about 24% compared to those in scenario *A*. As a result, by adopting ANM schemes more PV capacity can be accommodated and energy losses reduce compared to those in base case (passive networks).
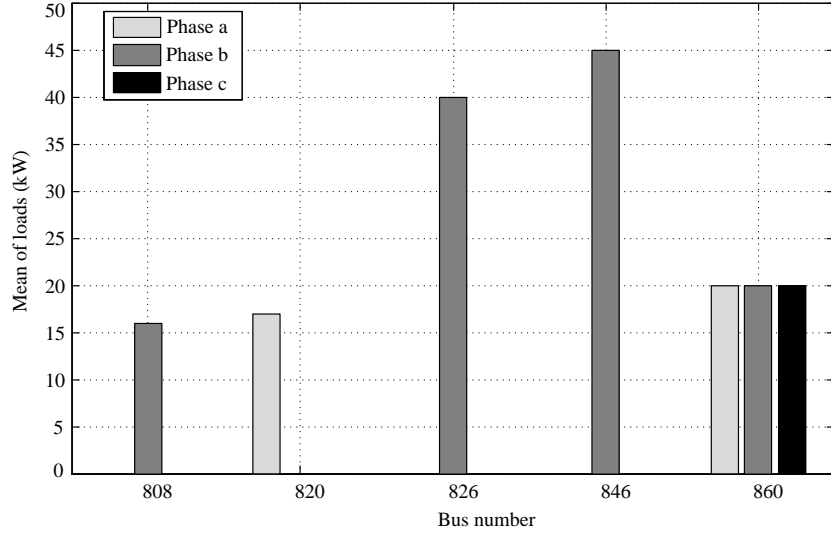
Table VI. The Mean of Energy Generated by PVs and Energy Losses in Different Scenarios

IEEE 13 bus test feeder				
Scenarios	Mean of total energy (MWh)	Mean of energy losses (kWh)	Energy generated increment (%)	Loss reduction (%)
A	3.69	48.13	-	-
B	3.88	42.51	5.15	11.68
C	4.51	38.75	22.22	19.49
IEEE 34 bus test feeder				
Scenarios	Mean of total energy (MWh)	Mean of energy losses (kWh)	Energy generated increment (%)	Loss reduction (%)
A	4.77	230.11	-	-
B	5.08	201.64	6.50	13.22
C	6.19	183.29	29.77	23.82

Figs. 8 (a), (b) show the mean of energy generated by PVs in scenario *C* and mean of loads at candidate buses. It is seen that bus 808 and phase b has the lowest dispatched energy compared to that at other buses due to the lowest amount of load at this phase. The dispatched energy at bus 860 at all phases is almost the same. This is because of the almost equal amount of the mean of loads at all phases which is shown in Fig.8 (b).
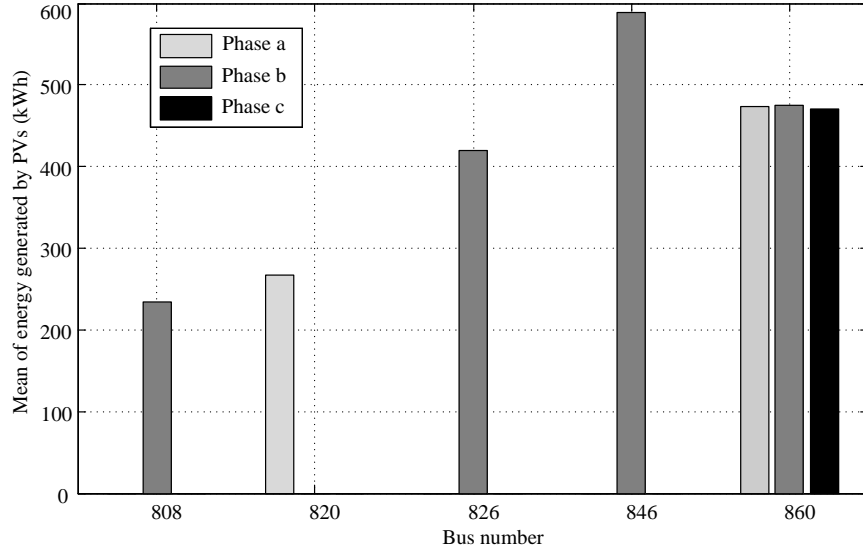
(a)

(b)

Fig.8. (a) Mean of energy generated by PVs at each phase and candidate buses in scenario C, (b) Mean of three-phase unbalanced loads at some buses and each

phase

C. Comparing with Other Methods

The proposed method is compared with other methods, namely non-dominated sorting genetic algorithm (NSGA-II) [44] and weighting factor method [45] on IEEE 13-bus test system. Table VII presents the number of Pareto-optimal solutions found by each method, the values of OF_1, OF_2 and the running time of each algorithm. It is evident that with the proposed method the energy generated by PVs (OF_1) is higher and the energy losses (OF_2) is lower than those obtained by weighting factor and NSGA II methods. Also, the computation time with the proposed method is less than that of the other methods.

Note that the results obtained by the proposed method are the best solutions (optimal) while with weighting factor method, the results are not optimal and we have chosen the closest results (in Table VII) to the ones obtained by the proposed method. NSGAII has some disadvantages as follows.

The first one is that individuals may be repeated numerously in a new population, since they belong to a higher-rank set. Another one is that, if the size of the first non-dominated set is bigger than the size of population then the convergence decreases and individuals tend to an extremum value of objective functions. However, the proposed method does not have these difficulties.

Table VII. Performance comparison between the proposed method and other methods for IEEE 13-bus test feeder

Method	Number of Pareto-optimal solutions	OF_1 (MWh)	OF_2 (kWh)	Running time (min)
NSGA II	20	3.64	49.24	206.27
Weighting factor	22	3.62	50.02	195.67
Proposed method	**16**	**3.69**	**48.13**	**193.80**

D. Computational Issues

The optimization variables of the multi-objective optimization problem include vector:

$X = (V_{i,t}^p, \theta_{i,t}^p, P_{g,t}^p, Q_{g,t}^p, P_{b,t}^p, Q_{b,t}^p, \phi_{g,t}^p, T_{ij}^p)$ where $p \in \{a,b,c\}$. The computational time required for solving the proposed method

for case studies *A* and *B* are about 3 and 5 hours, respectively. The problem characteristic is provided in Table VIII.

TableVIII. Problem characterization

Test System	IEEE 13-bus test feeder	IEEE 34-bus test feeder
Variables	12695	35754
Constraints	16962	48438
Time (min)	193.80	290.64

7. Conclusions

In this paper, a probabilistic methodology based on MCS technique for the operation of three-phase distribution networks considering ANM schemes including CVC and PFC is proposed. The method jointly maximizes the amount of energy generated by PVs and minimizes total energy losses of the lines from the point of view of DNOs over a year taking into account three-phase distribution network components modelling, uncertainties and network constraints. The stochastic nature of solar irradiance and unbalanced load demand are modelled by PDFs. MCS is utilized to use the generated PDFs and the ε-constraint method is used to solve the multi-objective optimization problem. Fuzzy satisfying approach is employed to select the best solution from the Pareto

optimal set. Even though the ANM schemes presented here reveal a major effect on increasing injection volumes of renewable DGs and reducing active power loss, their implementation will rely on proper regulatory incentives. For instance, DNOs receive a return on their assets but with ANM no extra assets are needed to indicate a disincentive for ANM schemes. The combination of the proposed method with the ANM schemes makes it a unique tool and its application shows the benefits of ANM. ANM is considered as an important means of increasing the capability of distribution networks to uptake renewable DGs. Results show that high penetration levels of PV generation capacity and loss reduction in three-phase distribution networks can be reached by properly implementing ANM schemes in comparison with the passive distribution networks. The proposed probabilistic method can assist DNOs in evaluating the impact of PV penetration on a given network in terms of technical performances and benefits. Moreover, it can help DG-owning DNOs to make a better decision to integrate the PVs into distribution networks.

Appendix A

Fuzzy satisfying (or max (min)) method is a popular technique for selection of the best solution among the obtained N_p Pareto optimal solutions. Suppose we have a problem with N objectives to be minimized. The linear membership function for the nth solution of the kth objective function is defined as [39]:

$$
\mu_k^n = \begin{cases} 1 & f_k^n \le f_k^{\min} \\ \dfrac{f_k^{\max} - f_k^n}{f_k^{\max} - f_k^{\min}} & f_k^{\min} \le f_k^n \le f_k^{\max} \\ 0 & f_k^n \ge f_k^{\max} \end{cases} \tag{26}
$$
$$
k = 1,\dots,N, \; n = 1,\dots,N_p
$$

where $f_k^{\max}$ and $f_k^{\min}$ are maximum and minimum values of the objective function k in solutions of Pareto optimal set. μ_k^n represents the optimality degree of the nth solution of the kth objective function. The membership function of nth solution can be calculated using the following equation:

$$
\mu^n = \min(\mu_1^n,\dots,\mu_N^n) \tag{27}
$$
$$
n = 1,\dots,N_p
$$

The solution with the maximum weakest membership function is the best solution. The corresponding membership function of this solution ($\mu_{\max}$), is calculated as follows:

$$
\mu_{\max} = \max(\mu^1,\dots,\mu^{N_p}) \tag{28}
$$

Acknowledgment

References

[1] *The Smart Grid: An Introduction*. [Online]. Available: http://www.oe.energy.gov/DocumentsandMedia/DOE_SG_Book_Single_Pages.pdf.

[2] F. Katiraei, K. Mauch, and L. Dignard-Bailey, "Integration of photovoltaic power systems in high-penetration clusters for distribution networks and mini-grids," *Int. J. Distrib. Energy Resources*, vol. 3, no. 3, pp. 207-224, 2007.

[3] M. Thomson and D. G. Infield, "Network power-flow analysis for a high penetration of distributed generation," *IEEE Trans. Power Syst.*, vol. 22, no. 3, pp. 1157-1162, Aug. 2007.

[4] A. Canova, L. Giaccone, F. Spertino, and M. Tartaglia, "Electrical impact of photovoltaic plant in distributed network," *IEEE Trans. Ind. Appl.*, vol. 45, no. 1, pp. 341-347, 2009.

[5] A. von Jouanne and B. Banerjee, "Assessment of voltage unbalance," *IEEE Trans. Power Del.*, vol. 16, no. 4, pp. 782-790, 2001.

[6] P. Juanuwattanakul and M. A. S. Masoum, "Voltage stability enhancement for unbalanced multiphase distribution networks," in *Proc. 2011 IEEE Power and Energy Society General Meeting*, Jul. 2011, pp.1-6.

[7] S. Tong, K. Nan Miu, "A network-based distributed slack bus model for DGs in unbalanced power flow studies", *IEEE Trans. Power Syst.*, vol. 20, no. 2, pp. 835-842, 2005.

[8] X.P. Zhang, P. Ju, E. Handschin, "Continuation three-phase power flow: a tool for voltage stability analysis of unbalanced three-phase power systems", *IEEE Trans. Power Syst.*, vol. 20, no. 3, pp. 1320-1329, 2005.

[9] X.P. Zhang, H. Chen, "Asymmetrical three-phase load-flow study based on symmetrical component theory", *IEE Proc. Gener. Transm. Distrib.*, vol. 141, no. 3, pp. 248-252, 1994.

[10] M.J.E. Alam, K. M. Muttaqi, and D. Sutanto, "A Three-phase power flow approach for integrated 3-wire MV and 4-wire multigrounded LV networks with rooftop solar PV", *IEEE Trans. Power Syst.*, vol. 28, no. 2, pp. 1728-1737, 2013.

[11] F. C. Lu and Y. Y. Hsu, "Fuzzy dynamic programming approach to reactive power/voltage control in a distribution substation," *IEEE Trans. Power Syst.*, vol. 12, no. 2, pp. 681–688, 1997.

[12] E. Dall'Anese, G.B. Giannakis, B.F. Wollenberg, "Economic dispatch in unbalanced distribution networks via semidefinite relaxation", Online: http://arxiv.org/abs/1207.0048.

[13] L.R.Araujo, D.R.R.Penido, F.A.Vieira, "A multiphase optimal power flow algorithm for unbalanced distribution systems", *Int. J. Elect. Power & Energy Syst.*, vol. 53, pp. 632-642, 2013.

[14] Y. Cao, Y. Tan, C. Li, C. Rehtanz, "Chance-constrained optimization-based unbalanced optimal power flow for radial distribution networks", *IEEE Trans. Power Syst.*, vol.28, no.3, pp. 1855-1864, 2013.

[15] S. Paudyal, C.A. Canizares, K. Bhattacharya, "Optimal operation of distribution feeders in smart grids", *IEEE Trans. Ind. Electronics*, vol. 58, no.10, pp.4495-4503, 2011.

[16] M.M.A. Abdelaziz, E.F. El-Saadany, "Maximum loadability consideration in droop-controlled islanded microgrids optimal power flow", *Elect Power Syst. Res.*, vol.106, pp.168-179, 2014.

[17] G.K. Viswanadha Raju and P.R. Bijwe, "Efficient reconfiguration of balanced and unbalanced distribution systems for loss minimisation", *IET Gener. Transm. Distrib.,* vol. 2, no.1, pp.7-12, 2008.

[18] M. Z. Kamh and R.Iravani, "Unbalanced model and power-flow analysis of Microgrids and active distribution systems", *IEEE Trans. Power Del.*, vol. 25, no. 4, pp. 2851-2858, 2010.

[19] Y. Y. Hsu and F. C. Lu, "A combined artificial neural network-fuzzy dynamic programming approach to reactive power/voltage control in a distribution substation," *IEEE Trans. Power Syst.*, vol. 13, no. 4, pp. 1265–1271, 1998.

[20] I. Roytelman, B. K. Wee, and R. L. Lugtu, "Volt/var control algorithm for modern distribution management system," *IEEE Trans. Power Syst.*, vol. 10, no. 3, pp. 1454–1460, 1995.

[21] M. Liu, S. K. Tso, and Y. Cheng, "An extended nonlinear primal-dual interior-point algorithm for reactive-power optimization of large-scale power systems with discrete control variables," *IEEE Trans. Power Syst.*, vol. 17, no. 4, pp. 982–991, 2002.

[22] M. B. Liu, C. A. Cañizares, and W. Huang, "Reactive power and voltage control in distribution systems with limited switching operations," *IEEE Trans. Power Syst.*, vol. 24, no. 2, pp. 889–899, 2009.

[23] D.Q. Hung, N. Mithulananthan, and K.Y. Lee, "Determining PV penetration for distribution systems with time-varying load models", *IEEE Trans. Power Syst.*, vol. 29, no.6, pp. 3048-3057, 2014.

[24] [Online]. Available: https://solaranywhere.com/Public/SelectData.aspx

[25] G. Mokryani, P. Siano, "Combined Monte Carlo simulation and OPF for wind turbines integration into distribution networks", *Electr. Power Syst. Res.*, vol.103, pp.37-48, 2013.

[26] P. Siano, G. Mokryani, "Probabilistic Assessment of the Impact of Wind Energy Integration into Distribution Networks", *IEEE Trans. Power Syst.*, vol.28, no.4, pp. 4209-4217, 2013.

[27] P.A.N. Garcia, J.L.R. Pereira and S.Jr. Cameiro "Voltage control devices models for distribution power flow analysis", *IEEE Trans. Power Syst.*, vol.16, no.4, pp. 586-594, 2001.

[28] P. Kundur, *Power System Stability and Control*, EPRI Power Engineering Series, McGraw-Hill, 1994.

[29] W.H. Kersting, *Distribution System Modeling and Analysis*, CRC Press, 2007.

[30] F. Youcef, A. Mefti, A. Adane, M.Y. Bouroubi, "Statistical analysis of solar measurements in Algeria using beta distributions", *Renew. Energy*, vol. 26, no.1, pp. 47-67, 2002.

[31] [Online] Available http://solar.org.au/papers/00papers/Caliao.PDF

[32] Z. M. Salameh, B. S. Borowy, and A. R. A. Amin, "Photovoltaic module-site matching based on the capacity factors," *IEEE Trans. Energy Convers.*, vol. 10, no. 2, pp. 326–332, 1995.

[33] R. Chedid, H. Akiki, S. Rahman, "A decision support technique for the design of hybrid solar-wind power systems", *IEEE Trans. Energy Convers.*, vol.13, no. pp. 76-83, 1995.

[34] Z. Fikri, "Statistical load analysis for distribution network planning," Ph.D. dissertation, Dept. Elect. Power Syst. Eng., Royal Inst. Technol., Stockholm, Sweden, 1975.

[35] P. Djapic, C. Ramsay, D. Pudjianto, G. Strbac, J. Mutale, N. Jenkins, and R. Allan, "Taking an active approach," *IEEE Power and Energy Mag.*, vol. 5, no. 4, pp. 68–77, 2007.

[36] L.F. Ochoa, C.J. Dent, and G.P. Harrison, "Distribution network capacity assessment: variable DG and active networks," *IEEE Trans. Power Syst.*, vol.25, no.1, pp. 87-95, 2010.

[37] L. F. Ochoa, A. Keane, and G. P. Harrison, "Minimizing the reactive support for distributed generation: Enhanced passive operation and smart distribution networks," *IEEE Trans. Power Syst.*, vol. 26, no. 4, pp. 2134–2142, 2011.

[38] [Online] Available at: http://www.ferc.gov/industries/electric/indus-act/market-planning/opf-papers/acopf-1-history-formulation-testing.pdf.

[39] K. Deb, *Multi-Objective Optimization Using Evolutionary Algorithms*. New York, NY, USA: Wiley, 2001, vol. 16.

[40] [Online]. Available: http://ewh.ieee.org/soc/pes/dsacom/testfeeders/.

[41] Integration of Storage in Electrical Distribution Systems and its Impact on the Depth of Penetration of DG. [Online]. Available: http:// canmetenergy-canmetenergie.nrcan-rncan.gc.ca/fichier.php/codectec/En/ 2009-174/2009-174.pdf.

[42] A. Brooke, D. Kendrick, A. Meeraus, R. Raman, "GAMS A User's Guide", GAMS Development Corporation, Washington DC, 1998.

[43] R. H. Byrd, J. Nocedal, and R. A. Waltz, "KNITRO: An integrated package for nonlinear optimization," in *Large-Scale Nonlinear Optimization*. New York: Springer-Verlag, pp. 35-59, 2006.

[44] K. Deb, A. Pratap, A. Agarwal, and T. Meyarivan, "A fast and elitist multi-objective genetic algorithm: NSGA II," *IEEE Trans. Evol. Comput.*, vol. 6, no. 2, pp. 182–197, Apr. 2002.

[45] I.Y. Kim, "Adaptive weighted sum method for multiobjective optimization" [Online] Available at:

http://web.mit.edu/deweck/www/PDF_archive/2%20Refereed%20Journal/2_12_SMO_AWSMOO1_deWeck_Kim.pdf.